N72-27273

NASA TECHNICAL MEMORANDUM

NASA TM X-64664

DESIGN OF A MACH 8.0 AXISYMMETRIC NOZZLE FOR A HYPERSONIC TEST FACILITY

By Joseph L. Sims and Robert F. Elkin
Aero-Astrodynamics Laboratory

May 24, 1972

NASA

George C. Marshall Space Flight Center
Marshall Space Flight Center, Alabama

MSFC - Form 3190 (Rev June 1971)

TECHNICAL REPORT STANDARD TITLE PAGE

1. REPORT NO. NASA TM X-64664	2. GOVERNMENT ACCESSION NO.	3. RECIPIENT'S CATALOG NO.
4. TITLE AND SUBTITLE DESIGN OF A MACH 8.0 AXISYMMETRIC NOZZLE FOR A HYPERSONIC TEST FACILITY		5. REPORT DATE May 24, 1972 6. PERFORMING ORGANIZATION CODE
7. AUTHOR(S) Joseph L. Sims and Robert F. Elkin		8. PERFORMING ORGANIZATION REPORT #
9. PERFORMING ORGANIZATION NAME AND ADDRESS George C. Marshall Space Flight Center Marshall Space Flight Center, Alabama 35812		10. WORK UNIT NO. 11. CONTRACT OR GRANT NO.
12. SPONSORING AGENCY NAME AND ADDRESS NASA Washington, D. C.		13. TYPE OF REPORT & PERIOD COVERED TECHNICAL MEMORANDUM 14. SPONSORING AGENCY CODE
15. SUPPLEMENTARY NOTES		

16. ABSTRACT

An axisymmetric nozzle has been designed to produce test section flow at a Mach number of 8.0 for use in a hypersonic test facility at MSFC. Nominal design conditions used to calculate the viscous correction to the wall contour were selected from the results of a parametric boundary layer investigation so that the widest possible range of satisfactory operating conditions could be obtained. Coordinates for the nozzle are presented in a tabular form suitable for design and manufacturing. The basic analysis techniques have been used to generate results to compare with experimental data from a facility at Langley Research Center. The agreement was reasonably good.

17. KEY WORDS	18. DISTRIBUTION STATEMENT Unclassified-Unlimited E. D. Geissler E. D. GEISSLER Director, Aero-Astrodynamics Lab, MSFC

19. SECURITY CLASSIF. (of this report) Unclassified	20. SECURITY CLASSIF. (of this page) Unclassified	21. NO. OF PAGES 23	22. PRICE $3.00

MSFC - Form 3292 (May 1969)

DEFINITION OF SYMBOLS

a^*	Critical speed of sound
E	Nozzle exit
V	Velocity
P	Pressure
R_o	Circular arc radius of curvature for the downstream throat region of the conical nozzle (Sketch B)
T	Temperature
x,r	Longitudinal and radial coordinates of the cylindrical coordinate system
δ	Boundary layer velocity thickness
δ^*	Boundary layer displacement thickness
ρ_s	Circular arc radius of curvature for the nozzle wall contour upstream of the throat (Sketch A)
θ	Boundary layer momentum thickness

<u>Subscripts</u>

o	Stagnation conditions
t	Throat conditions
w	Wall conditions

DESIGN OF A MACH 8.0 AXISYMMETRIC NOZZLE FOR A HYPERSONIC TEST FACILITY

SUMMARY

An axisymmetric nozzle has been designed to produce test section flow at a Mach number of 8.0 for use in a hypersonic test facility at MSFC. Nominal design conditions used to calculate the viscous correction to the wall contour were selected from the results of a parametric boundary layer investigation so that the widest possible range of satisfactory operating conditions could be obtained. Coordinates for the nozzle are presented in tabular form suitable for design and manufacturing. The basic analysis techniques have been used to generate results to compare with experimental data from a facility at Langley Research Center. The agreement was reasonably good.

INTRODUCTION

An axisymmetric nozzle for a hypersonic test facility at MSFC has been designed to produce a test section Mach number of 8.0 when operated at nominal design conditions. The nominal conditions were selected from the results of a parametric investigation of the effects of stagnation pressure, stagnation temperature, and wall temperature upon the boundary layer correction to the inviscid nozzle coordinates.

These coordinates were obtained from a method-of-characteristics computer program devised at MSFC. This program, starting from an initial value line obtained from a transonic solution and using a prescribed nozzle centerline velocity distribution as a boundary condition, computes the entire nozzle shape downstream of the throat. The transonic solution that was used is valid only for a circular arc approaching the throat from the subsonic side. Thus, the contour of a portion of the subsonic side is shaped by the transonic solution requirements. The remainder of the subsonic side was shaped to minimize the possibility of thermal stratification and to maintain compatibility with the requirements of lower Mach number nozzles.

A turbulent boundary layer program using an integral solution technique was used to obtain the viscous correction to the inviscid nozzle coordinates. The adequacy of the combination of these two programs has been demonstrated previously for lower Mach number nozzles. Included herein is a comparison of calculated boundary layer results with experimental data from the Langley Research Center Mach 6 hypersonic tunnel. The agreement between the two types of data is satisfactory. Since there should be virtually no Mach number effects on the accuracy of the inviscid solution, it is anticipated that the nozzle will produce a satisfactory flow field for test purposes.

ANALYSIS AND RESULTS

The analysis that was applied to compute the supersonic side inviscid coordinates of the nozzle was the axisymmetric method of characteristics. In formulating a computer program to apply this method, which is a point-by-point solution of the entire supersonic portion of the flow field, initial conditions, centerline boundary conditions, and final Mach line boundary conditions must be specified. These conditions, as illustrated in sketch A, were specified in the following manner for the computer program used to generate the numerical results.

The location of the initial value line and the numerical value of the flow variables along the line were obtained from the transonic solution in reference 1. Briefly, this solution is obtained by using a power series expansion in the equation of motion and solving for the unknown coefficients in terms of the radius of curvature of the nozzle wall, which is assumed to be a circular arc. This solution should be most accurate for nozzles which have a large radius of curvature compared with the throat radius. For this reason, a value of $\rho_s/r_t = 10.0$ was selected.

The centerline velocity distribution must be specified from point 1 (sketch A), whose location and velocity value are specified by the transonic solution, to point 2, which has a somewhat arbitrary location, but has the specified design velocity. This velocity distribution may be specified in the program by a polynomial equation which has coefficients defined by input data or it may be defined point by point as input data. For this study, the latter procedure was selected since it offered two significant advantages in the hypersonic case: (1) The step size along the centerline can be variable in order to achieve maximum accuracy of the solution. (2) A velocity distribution can be obtained which restricts the maximum wall angle to any desired value. This technique can be used to obtain small wall angles to minimize start time. The major problem with specifying the centerline velocity distribution in this manner is the additional time and effort it requires.

The centerline velocity distribution used for this design study was obtained by computing the flow field in a nozzle which consisted of a circular arc downstream of the throat followed by a ten-degree conical nozzle tangent to the circular arc at the point of intersection. This shape, shown in sketch B, was selected after a flow field analysis of several contours with different shapes leading up to the conical section. A value of 20 r_t was selected for the circular arc radius of curvature; the flow field studies proved that this was sufficient to prevent the formation of a shock from the arc-cone juncture.

SKETCH A

ILLUSTRATION OF BOUNDARY CONDITIONS

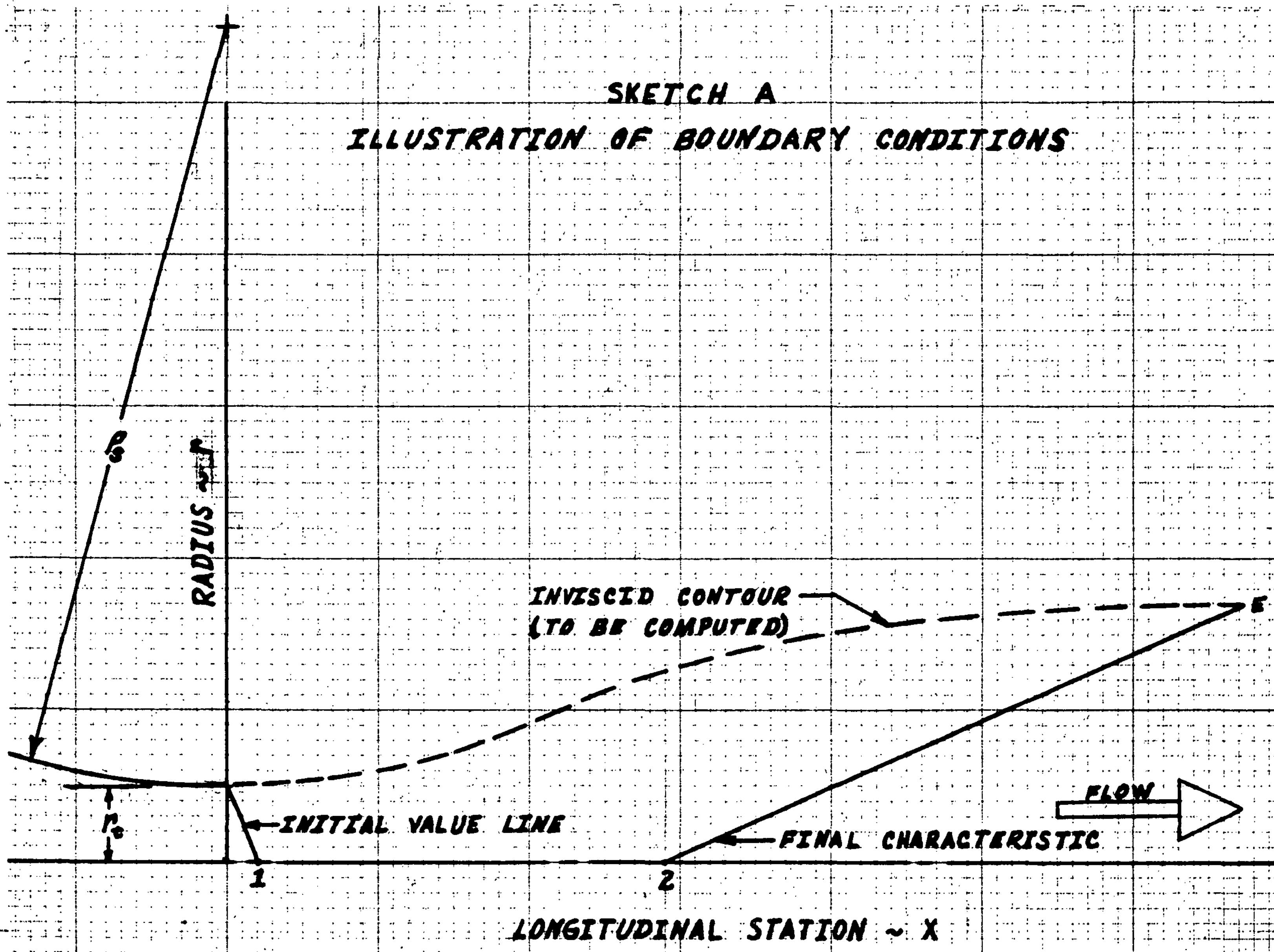

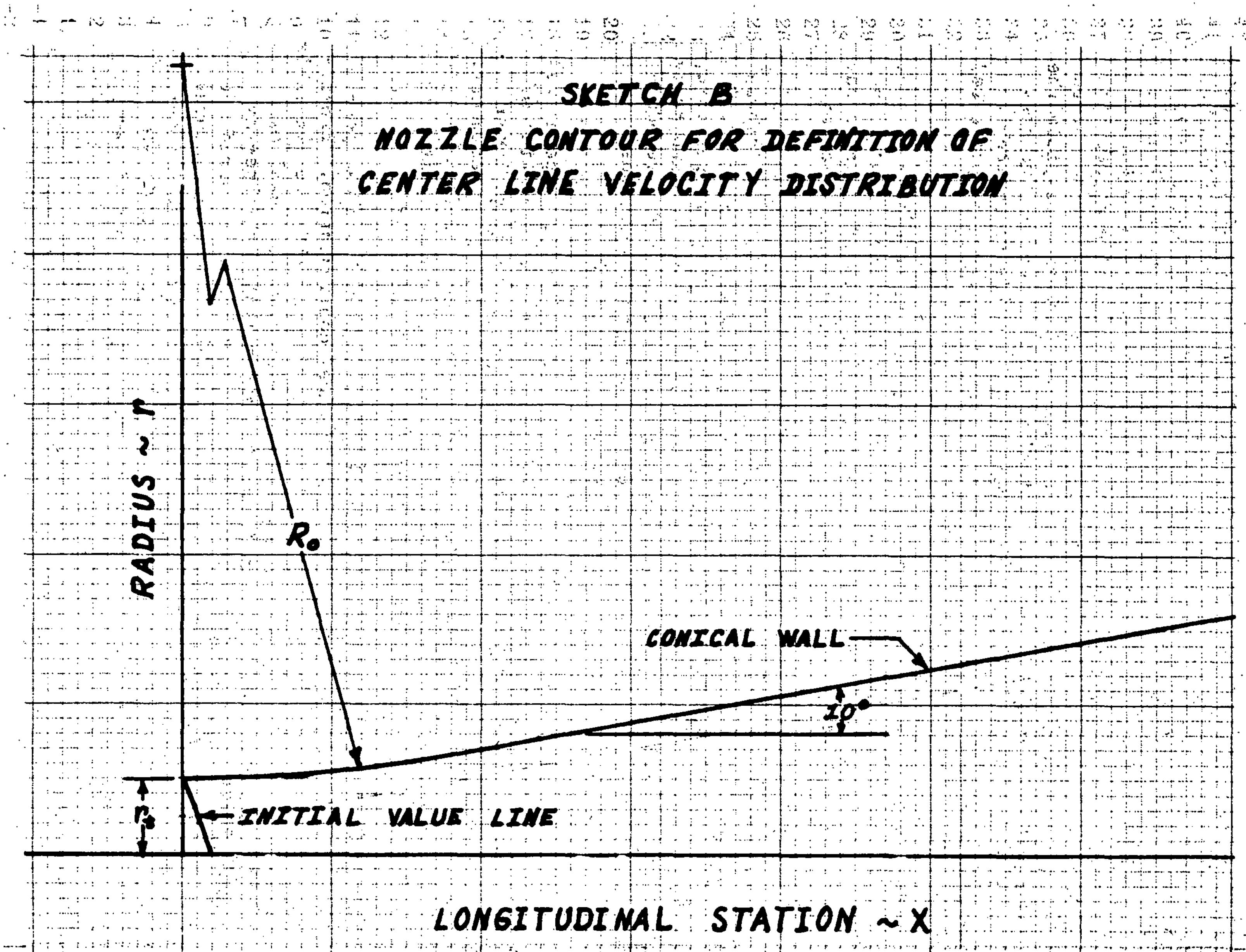

SKETCH B

NOZZLE CONTOUR FOR DEFINITION OF CENTER LINE VELOCITY DISTRIBUTION

Calculations performed in the nozzle design deck require that the derivative of the centerline velocity be known. This was obtained by numerically differentiating the data obtained from the conical nozzle flow field solution. The final derivative function shown in figure 1 was a composite of this curve and a linear, constant slope section tangent to the numerical function and extending to a value of zero for the derivative. Selection of the point of tangency was governed by the requirement that the integral of the derivative function must yield the design velocity at the longitudinal station where the derivative goes to zero. The velocity distribution resulting from this composite derivative function, which was used in the design program, is presented in figure 2.

The boundary layer growth analysis is essentially the same as that derived by Elliot, Bartz and Silver (ref. 2). Their assumption of a 1/7th power velocity and temperature profiles in the boundary layer has been replaced by an arbitrary power determined from a correlation of experimental data.

Basically, the analysis is a simultaneous solution of the integral axisymmetric, compressible momentum and energy equations for an ideal gas. Standard definitions of the boundary layer velocity, temperature, and displacement thicknesses, along with the assumption of an arbitrary velocity and total temperature power profile, are used to derive additional equations to complete the boundary layer growth solutions. Constant pressure is assumed across the boundary layer.

The boundary layer power profiles (velocity and total temperature) are obtained from a correlation of experimental data as a function of momentum Reynolds number (ref. 4). Friction coefficients are taken from a correlation of adiabatic, incompressible flat-plate experimental data and corrected for compressibility and heat transfer effects by use of Eckert's reference temperature (refs. 5 and 6). Stanton number is obtained from the Von Karman incompressible equation.

As part of the design study, a boundary layer analysis was performed for the Langley Mach 6 hypersonic tunnel configuration. Experimental data obtained from the calibration of this facility are available in reference 3. Comparisons of the analytical and experimental displacement, total boundary layer (velocity) and momentum thicknesses are presented in figures 3, 4, and 5. Agreement between measured and analytical displacement and total boundary layer thicknesses (figures 3 and 4) is seen to be good. However, agreement between the two sets of momentum thicknesses (figure 5) is only fair in the downstream portion of the test section and is relatively poor in the upstream section.

Since the tunnel wall boundary layer description at a given axial location depends upon upstream conditions and since experimental data were not obtained for the converging-diverging section of the Mach 6 tunnel, the exact cause of the momentum thickness discrepancy could not be ascertained. However, there are two possible explanations. First, it was noted that the analytical and experimental velocity and temperature profiles through the boundary layer did not match in the upstream portion of the test section. This was due, in part at least, to the nonuniform temperature in the stagnation chamber reported in reference 2. Second, in calculating the analytical momentum thickness, the integral momentum equation was solved using a flat plate friction coefficient; whereas, the experimental data were obtained from the physical definition of momentum thickness using measured boundary layer properties.

Although these deficiencies in the momentum thickness comparison were observed, the overall comparison of the analytical and experimental data is good. Thus, it appears that use of the analytical displacement thickness to correct the inviscid coordinates will provide a satisfactory tunnel wall contour.

Figures 6 and 7 present the Mach 8 axisymmetric nozzle boundary layer displacement thickness and total thickness, respectively. These calculations are based on a nominal set of stagnation chamber values, which are noted on the figures. The nominal design values were selected after a parametric boundary layer study over the entire range of stagnation variables. Nominal values were selected that minimize the effect of deleterious boundary layer variations over the most useful operating range of the facility.

The coordinates for the entire curvilinear portion of the nozzle wall are given in table 1. All of the coordinates are given in inches and the throat has been used as the reference station for the longitudinal coordinates. These coordinates, which are the end result of the entire study, are the values that will be used for nozzle fabrication. The subsonic shape from the valve to the first ordinate listed in table 1 consists of cylindrical and conical tubes and are explicitly defined by appropriate design drawings.

CONCLUDING REMARKS

Analysis techniques incorporated in currently operational computer programs have been used to derive the nozzle contour for the design of a hypersonic test facility at MSFC. These analysis techniques have been verified through comparison with experimental data and calibration results from other nozzles designed by the same procedures. Therefore, it is anticipated that the current design will produce a flow field of satisfactory quality.

REFERENCES

1. Sims, Joseph L.: "Calculations of Transonic Nozzle Flow," NASA TM X-53081, October 12, 1964.

2. Elliot, D. M., D. R. Bartz and S. Silver: "Calculation of the Turbulent Boundary Layer Growth and Heat Transfer in Axisymmetric Nozzles," JPL Report No. 32-387, February 1963.

3. Jones, Robert A. and William V. Reller: "Preliminary Surveys of the Wall Boundary Layer in a Mach 6 Axisymmetric Tunnel," NASA TN D-5620, February 1970.

4. Persh, Jerome: "A Theoretical Investigation of Turbulent Boundary Layer Flow with Heat Transfer at Supersonic and Hypersonic Speeds," NAVORD Report 3854, May 1955.

5. Coles, Donald E.: "The Turbulent Boundary Layer in a Compressible Fluid," Rand Report No. P-2417, August 1961.

6. Eckert, E. R. G.: "Engineering Relations for Heat Transfer and Friction in High Velocity Laminar and Turbulent Boundary Layer Flow Over Surfaces with Constant Pressure and Temperature," Transactions of the ASME, Vol. 78, August 1956.

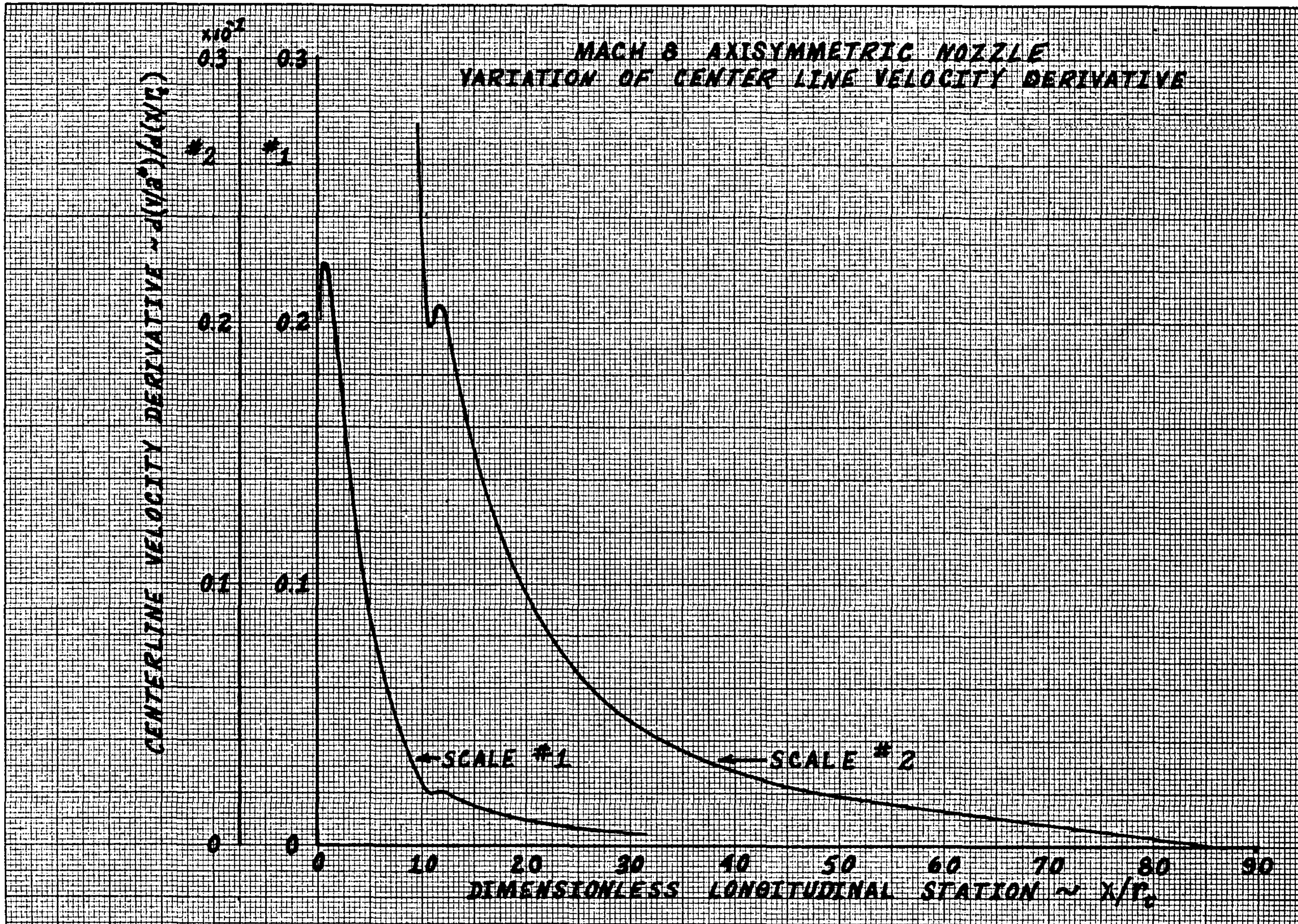
MACH 8 AXISYMMETRIC NOZZLE
VARIATION OF CENTER LINE VELOCITY DERIVATIVE
CENTERLINE VELOCITY DERIVATIVE ~ $d(V/a^*)/d(X/r_c)$
$\times 10^{-1}$
#2
#1
0.3
0.2
0.1
0
0
10
20
30
40
50
60
70
80
90
SCALE #1
SCALE #2
DIMENSIONLESS LONGITUDINAL STATION ~ X/r_c

FIGURE 1

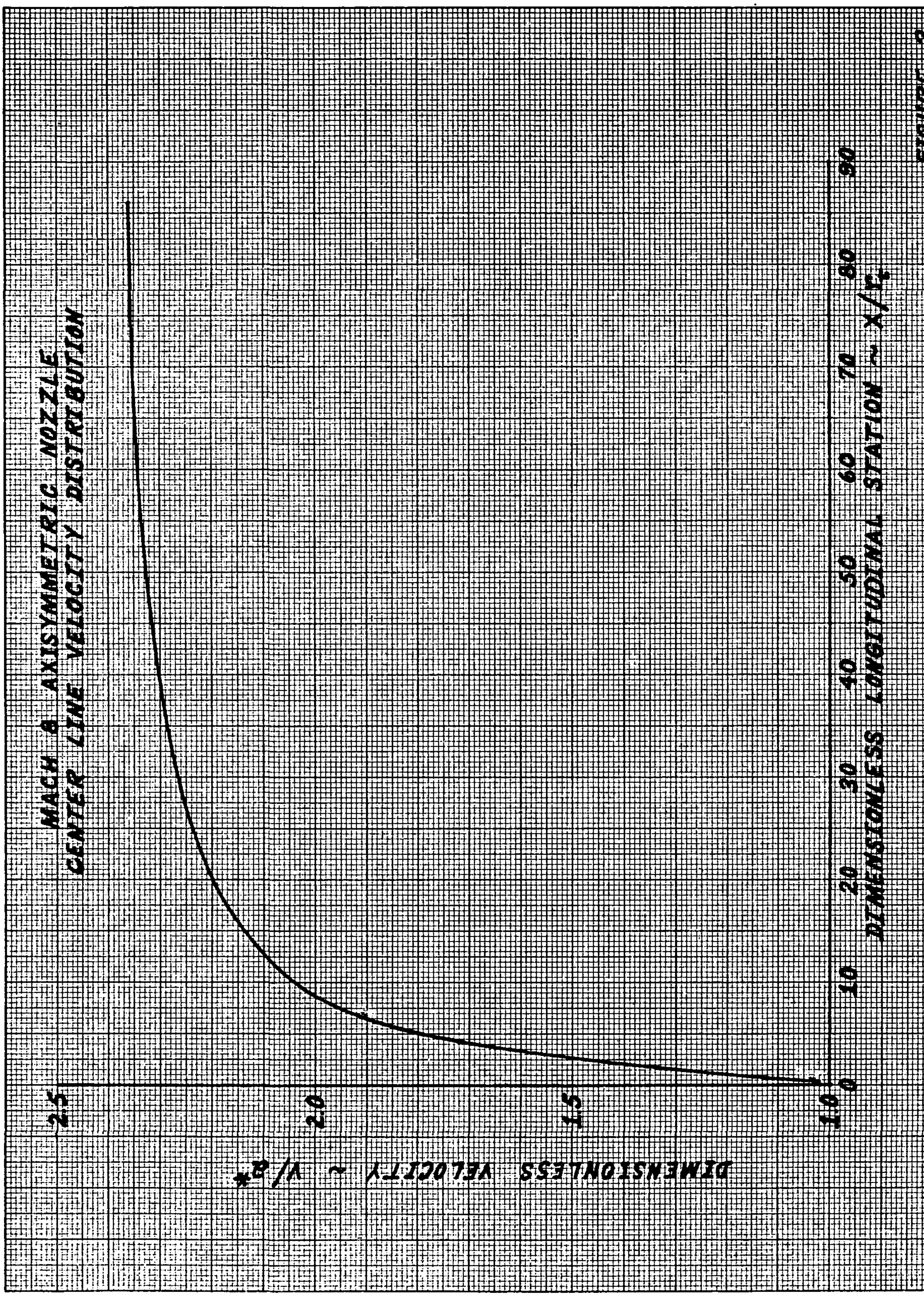
MACH 8 AXISYMMETRIC NOZZLE
CENTER LINE VELOCITY DISTRIBUTION
2.5
2.0
1.5
1.0
DIMENSIONLESS VELOCITY ~ V/a*
0
10
20
30
40
50
60
70
80
90
DIMENSIONLESS LONGITUDINAL STATION ~ X/r_t

FIGURE 2

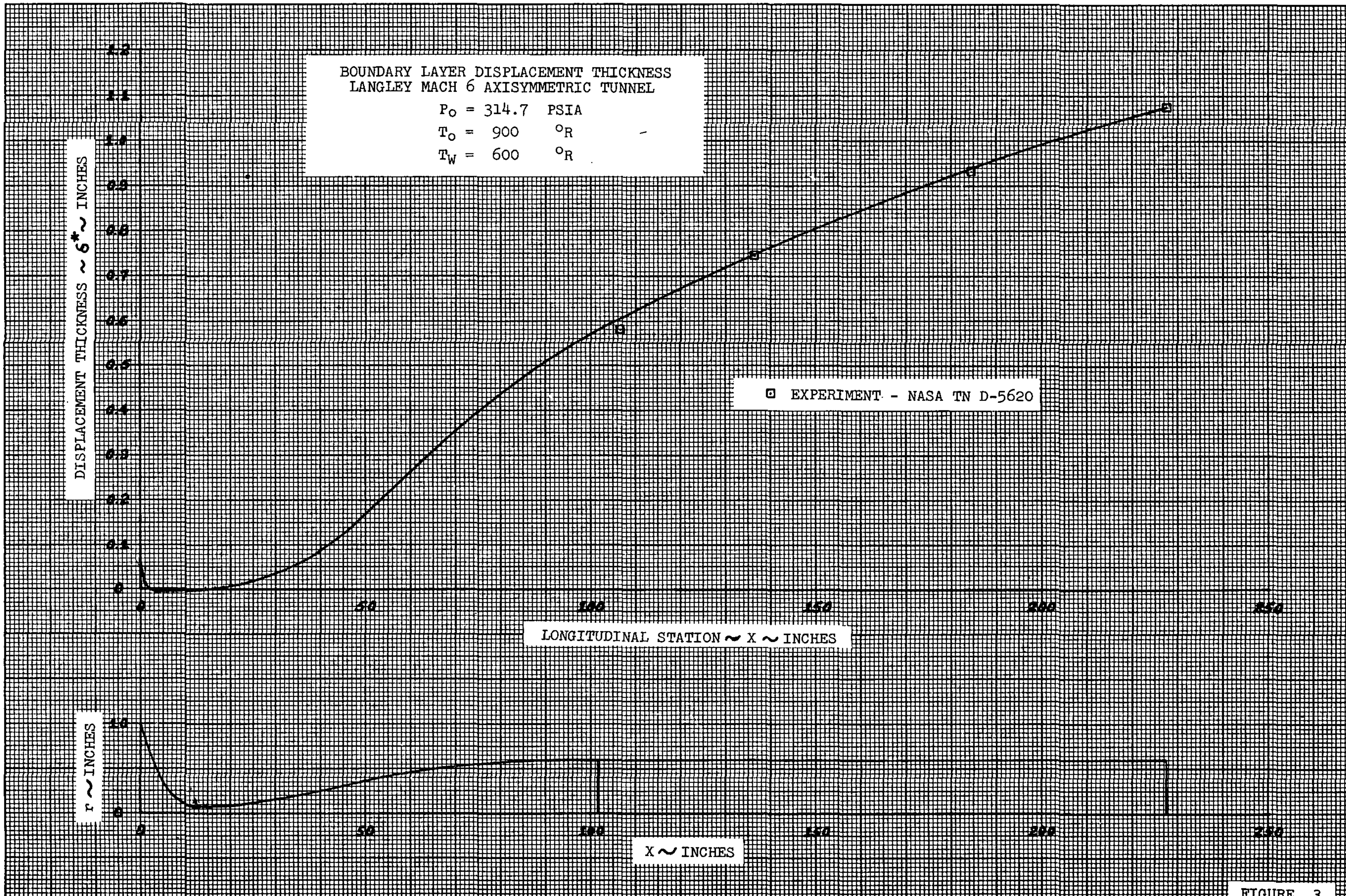
BOUNDARY LAYER DISPLACEMENT THICKNESS
LANGLEY MACH 6 AXISYMMETRIC TUNNEL
P_o = 314.7 PSIA
T_o = 900 °R
T_W = 600 °R
DISPLACEMENT THICKNESS ~ δ^* ~ INCHES
EXPERIMENT - NASA TN D-5620
LONGITUDINAL STATION ~ X ~ INCHES
r ~ INCHES
X ~ INCHES
0
50
100
150
200
250

FIGURE 3

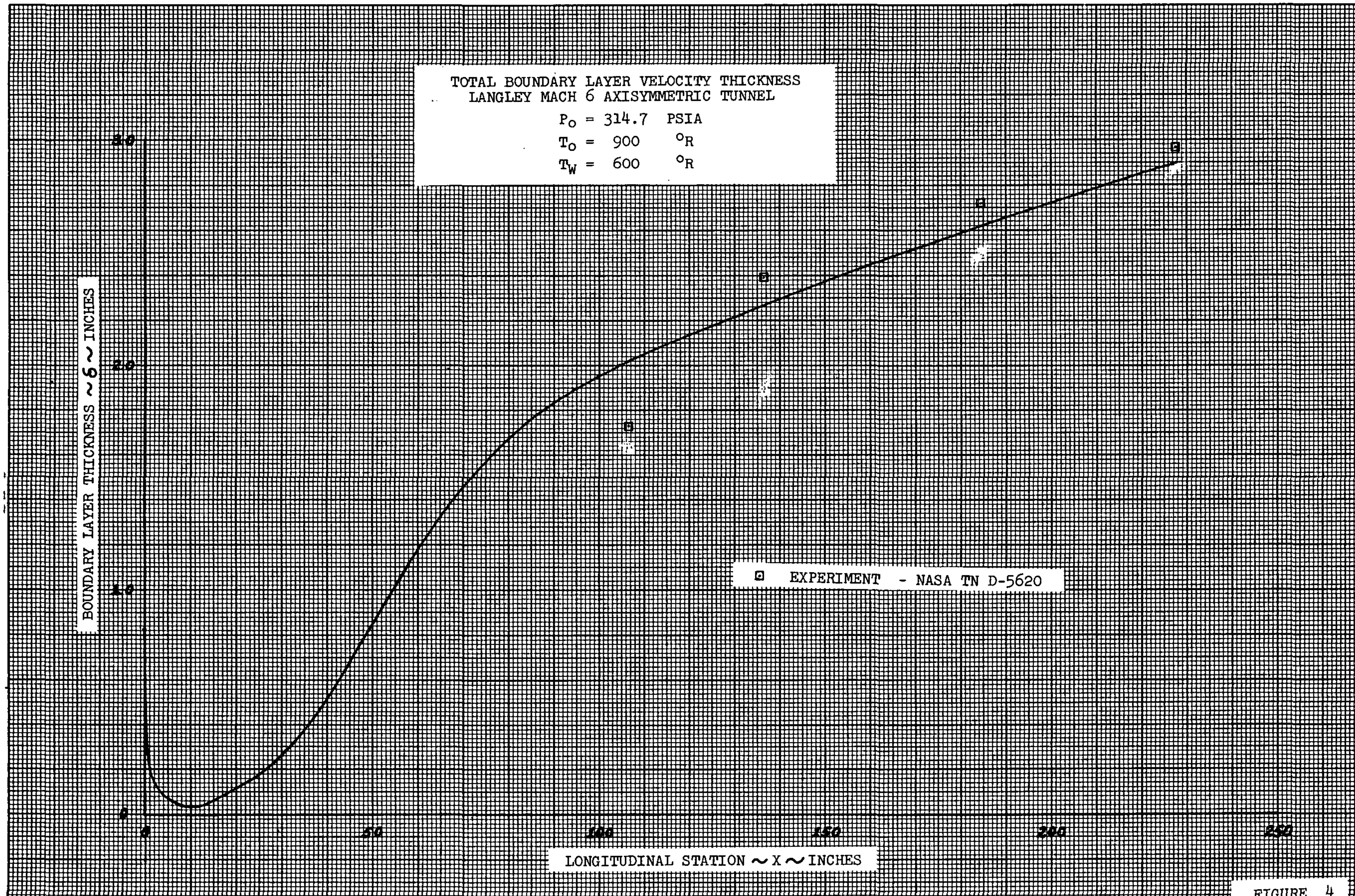
TOTAL BOUNDARY LAYER VELOCITY THICKNESS
LANGLEY MACH 6 AXISYMMETRIC TUNNEL
P_o = 314.7 PSIA
T_o = 900 °R
T_W = 600 °R
EXPERIMENT - NASA TN D-5620
BOUNDARY LAYER THICKNESS ~ δ ~ INCHES
LONGITUDINAL STATION ~ X ~ INCHES
0
1.0
2.0
3.0
0
50
100
150
200
250

FIGURE 4

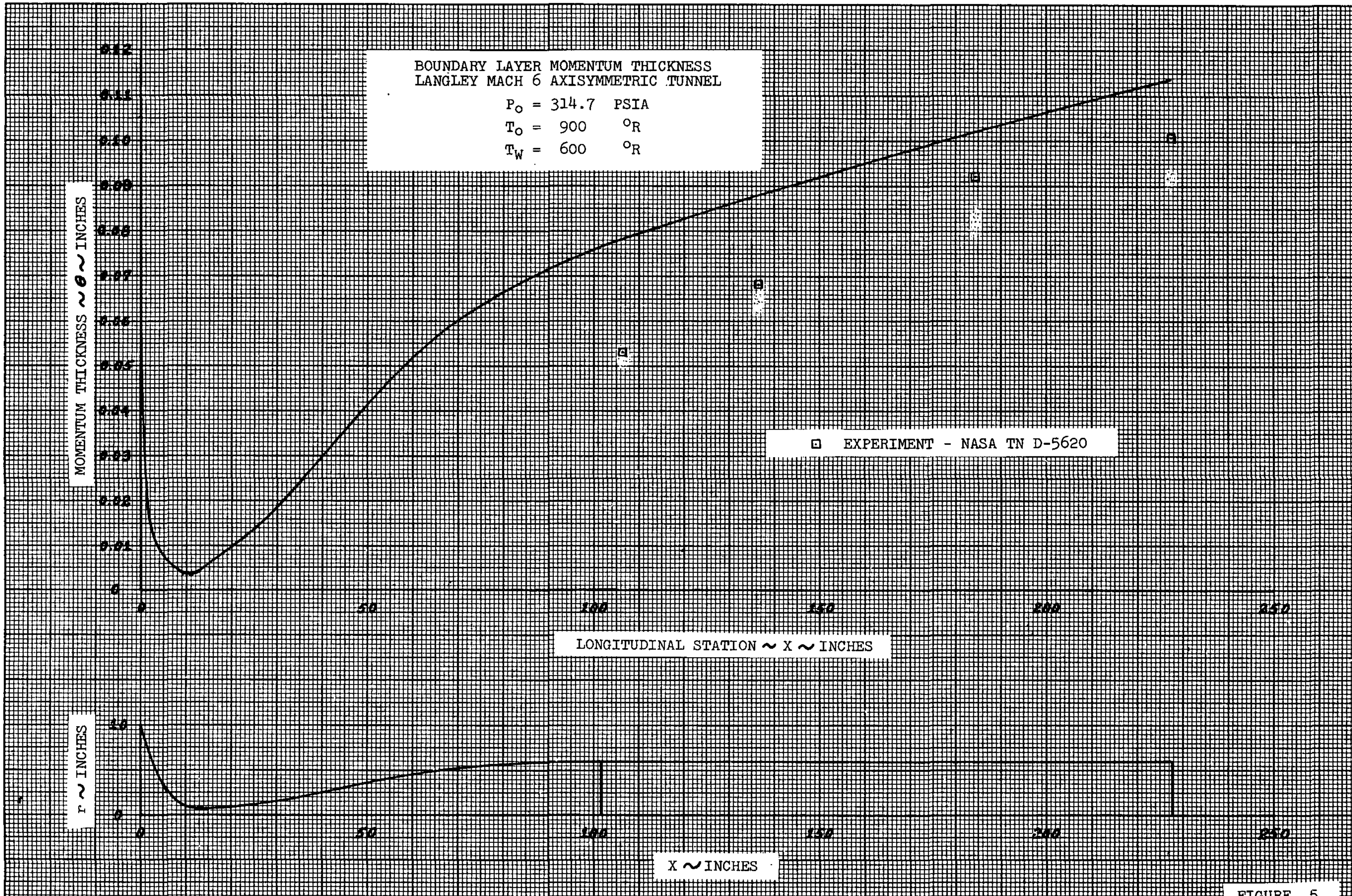

BOUNDARY LAYER MOMENTUM THICKNESS
LANGLEY MACH 6 AXISYMMETRIC TUNNEL
P_o = 314.7 PSIA
T_o = 900 °R
T_W = 600 °R
EXPERIMENT - NASA TN D-5620
MOMENTUM THICKNESS ~ θ ~ INCHES
0.12
0.11
0.10
0.09
0.08
0.07
0.06
0.05
0.04
0.03
0.02
0.01
0
0
50
100
150
200
250
LONGITUDINAL STATION ~ X ~ INCHES
r ~ INCHES
1.0
0
X ~ INCHES

FIGURE 5

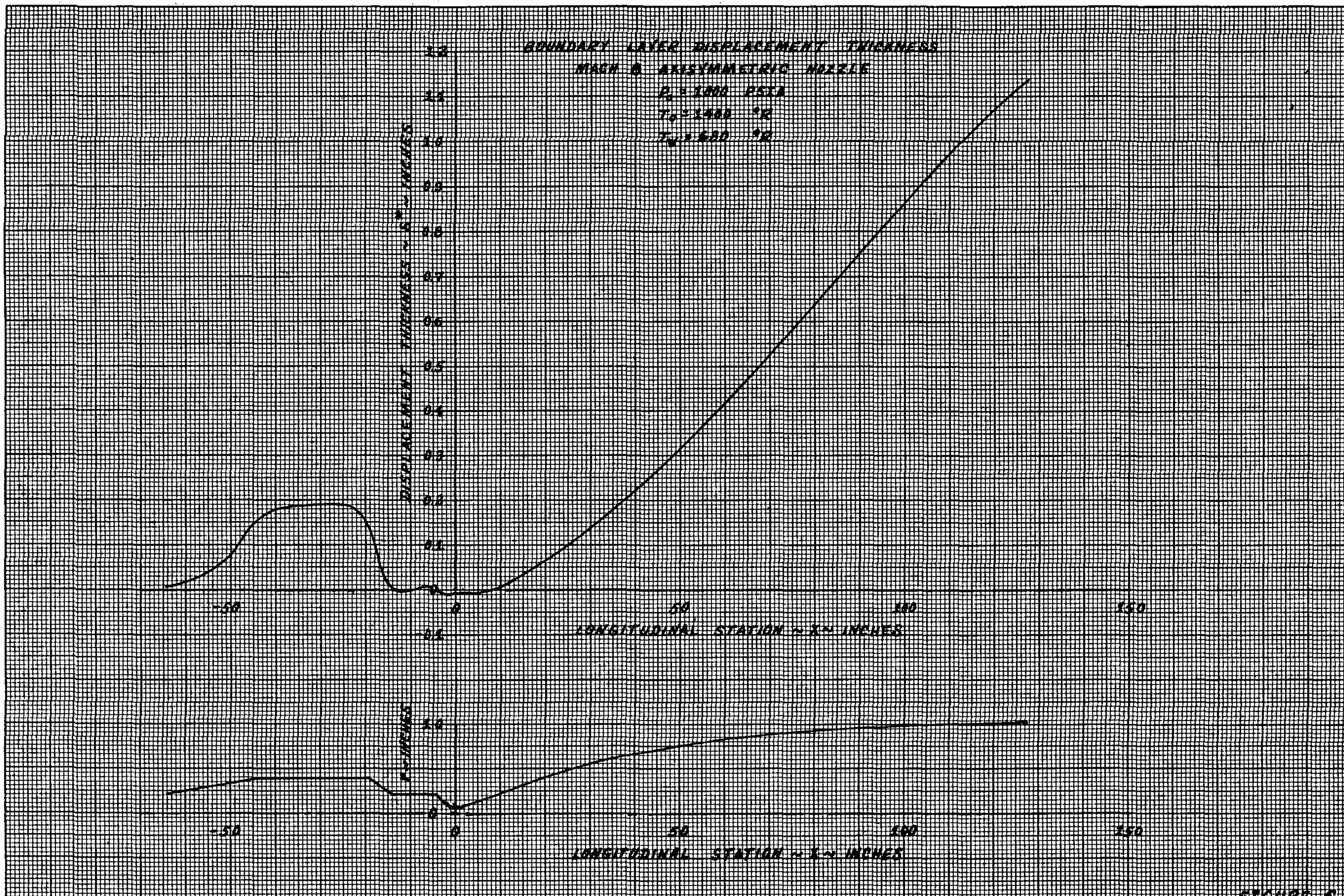
BOUNDARY LAYER DISPLACEMENT THICKNESS
MACH 8 AXISYMMETRIC NOZZLE
DISPLACEMENT THICKNESS ~ δ* ~ INCHES
LONGITUDINAL STATION ~ X ~ INCHES
r ~ INCHES
LONGITUDINAL STATION ~ X ~ INCHES

FIGURE 6

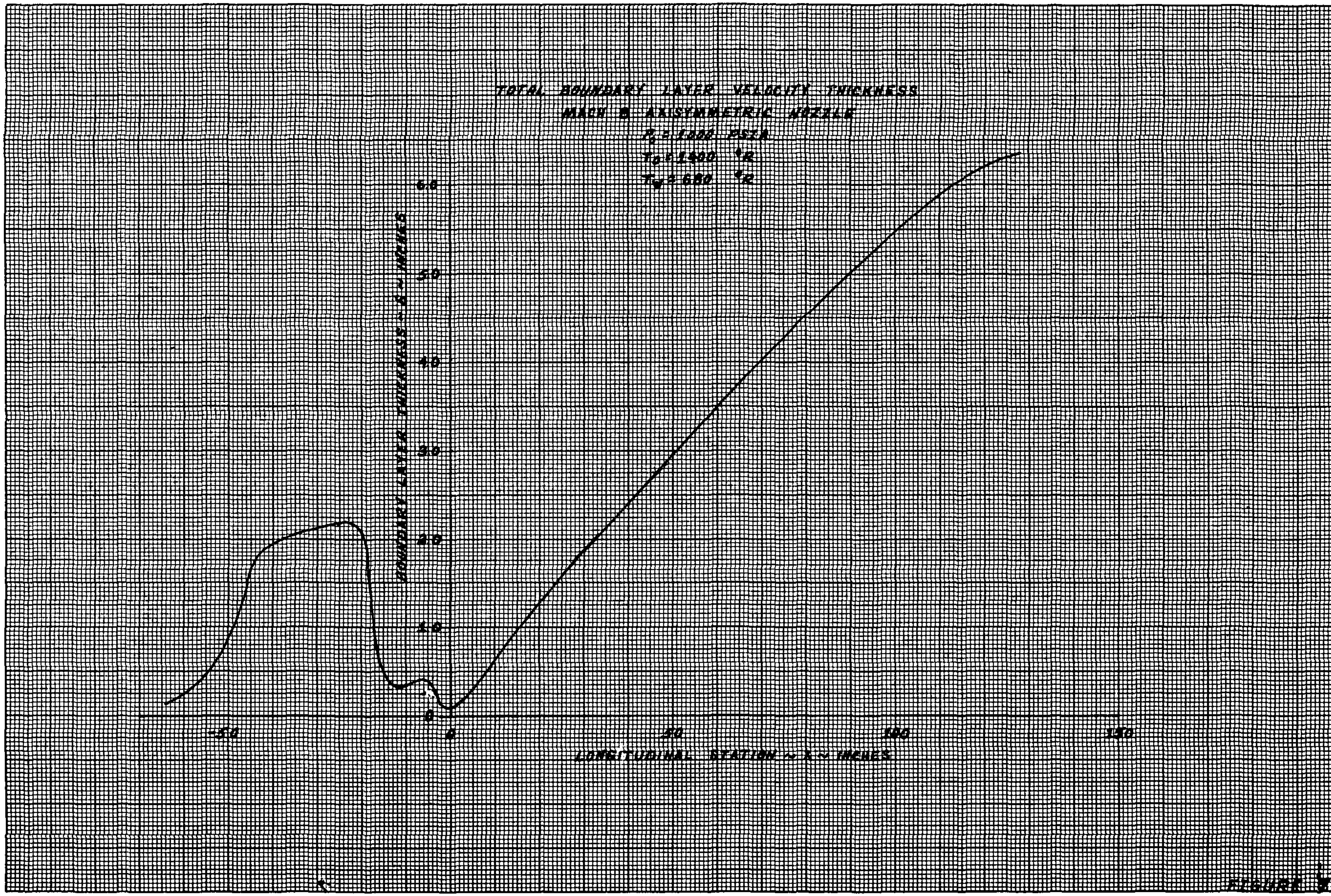
TOTAL BOUNDARY LAYER VELOCITY THICKNESS
MACH 8 AXISYMMETRIC NOZZLE
P_0 = 1000 PSIA
T_0 = 1400 °R
T_w = 680 °R
BOUNDARY LAYER THICKNESS ~ δ ~ INCHES
6.0
5.0
4.0
3.0
2.0
1.0
0
-50
0
50
100
150
LONGITUDINAL STATION ~ X ~ INCHES
FIGURE

TABLE 1

NOZZLE CONTOUR COORDINATES

X-INCHES	R-INCHES	X-INCHES	R-INCHES	X-INCHES	R-INCHES
-4.0610	2.0610	7.2500	1.7361	18.5000	3.7535
-3.7500	1.8338	7.5000	1.7805	18.7500	3.7958
-3.5000	1.6626	7.7500	1.8259	19.0000	3.8382
-3.2500	1.5092	8.0000	1.8700	19.2500	3.8804
-3.0000	1.3719	8.2500	1.9156	19.5000	3.9219
-2.7500	1.2489	8.5000	1.9600	19.7500	3.9637
-2.5000	1.1393	8.7500	2.0046	20.0000	4.0050
-2.2500	1.0420	9.0000	2.0506	20.2500	4.0459
-2.0000	0.9564	9.2500	2.0948	20.5000	4.0870
-1.7500	0.8819	9.5000	2.1396	20.7500	4.1275
-1.5000	0.8182	9.7500	2.1856	21.0000	4.1677
-1.2500	0.7648	10.0000	2.2302	21.2500	4.2082
-1.0000	0.7214	10.2500	2.2750	21.5000	4.2478
-0.7500	0.6880	10.5000	2.3212	21.7500	4.2874
-0.5000	0.6642	10.7500	2.3658	22.0000	4.3271
-0.2500	0.6500	11.0000	2.4107	22.2500	4.3660
0.0000	0.6453	11.2500	2.4567	22.5000	4.4049
0.2500	0.6487	11.5000	2.5015	22.7500	4.4437
0.5000	0.6581	11.7500	2.5467	23.0000	4.4821
0.7500	0.6733	12.0000	2.5926	23.2500	4.5202
1.0000	0.6936	12.2500	2.6377	23.5000	4.5583
1.2500	0.7186	12.5000	2.6833	23.7500	4.5960
1.5000	0.7471	12.7500	2.7284	24.0000	4.6335
1.7500	0.7795	13.0000	2.7741	24.2500	4.6707
2.0000	0.8154	13.2500	2.8192	24.5000	4.7078
2.2500	0.8536	13.5000	2.8649	24.7500	4.7448
2.5000	0.8945	13.7500	2.9100	25.0000	4.7812
2.7500	0.9369	14.0000	2.9557	25.2500	4.8176
3.0000	0.9807	14.2500	3.0008	25.5000	4.8539
3.2500	1.0248	14.5000	3.0462	25.7500	4.8898
3.5000	1.0690	14.7500	3.0913	26.0000	4.9253
3.7500	1.1128	15.0000	3.1366	26.2500	4.9608
4.0000	1.1579	15.2500	3.1816	26.5000	4.9961
4.2500	1.2018	15.5000	3.2266	26.7500	5.0311
4.5000	1.2456	15.7500	3.2714	27.0000	5.0659
4.7500	1.2906	16.0000	3.3161	27.2500	5.1005
5.0000	1.3346	16.2500	3.3608	27.5000	5.1350
5.2500	1.3792	16.5000	3.4051	27.7500	5.1693
5.5000	1.4241	16.7500	3.4495	28.0000	5.2031
5.7500	1.4676	17.0000	3.4933	28.2500	5.2368
6.0000	1.5126	17.2500	3.5373	28.5000	5.2704
6.2500	1.5573	17.5000	3.5809	28.7500	5.3038
6.5000	1.6024	17.7500	3.6244	29.0000	5.3369
6.7500	1.6461	18.0000	3.6676	29.2500	5.3697
7.0000	1.6910	18.2500	3.7105	29.5000	5.4025

TABLE 1 - CONT.
NOZZLE CONTOUR COORDINATES

X-INCHES	R-INCHES	X-INCHES	R-INCHES	X-INCHES	R-INCHES
29.7500	5.4352	41.0000	6.7112	52.2500	7.6852
30.0000	5.4675	41.2500	6.7359	52.5000	7.7040
30.2500	5.4995	41.5000	6.7604	52.7500	7.7227
30.5000	5.5314	41.7500	6.7848	53.0000	7.7413
30.7500	5.5632	42.0000	6.8090	53.2500	7.7598
31.0000	5.5948	42.2500	6.8330	53.5000	7.7782
31.2500	5.6262	42.5000	6.8569	53.7500	7.7965
31.5000	5.6572	42.7500	6.8806	54.0000	7.8146
31.7500	5.6881	43.0000	6.9041	54.2500	7.8327
32.0000	5.7190	43.2500	6.9276	54.5000	7.8506
32.2500	5.7496	43.5000	6.9509	54.7500	7.8684
32.5000	5.7800	43.7500	6.9741	55.0000	7.8861
32.7500	5.8102	44.0000	6.9972	55.2500	7.9037
33.0000	5.8402	44.2500	7.0201	55.5000	7.9212
33.2500	5.8700	44.5000	7.0429	55.7500	7.9386
33.5000	5.8998	44.7500	7.0655	56.0000	7.9558
33.7500	5.9293	45.0000	7.0880	56.2500	7.9730
34.0000	5.9586	45.2500	7.1103	56.5000	7.9901
34.2500	5.9876	45.5000	7.1325	56.7500	8.0071
34.5000	6.0166	45.7500	7.1546	57.0000	8.0240
34.7500	6.0454	46.0000	7.1766	57.2500	8.0407
35.0000	6.0741	46.2500	7.1984	57.5000	8.0574
35.2500	6.1025	46.5000	7.2202	57.7500	8.0740
35.5000	6.1308	46.7500	7.2418	58.0000	8.0905
35.7500	6.1588	47.0000	7.2633	58.2500	8.1069
36.0000	6.1867	47.2500	7.2846	58.5000	8.1232
36.2500	6.2145	47.5000	7.3057	58.7500	8.1393
36.5000	6.2421	47.7500	7.3266	59.0000	8.1554
36.7500	6.2696	48.0000	7.3477	59.2500	8.1714
37.0000	6.2968	48.2500	7.3685	59.5000	8.1873
37.2500	6.3238	48.5000	7.3892	59.7500	8.2031
37.5000	6.3507	48.7500	7.4097	60.0000	8.2188
37.7500	6.3775	49.0000	7.4302	60.2500	8.2344
38.0000	6.4041	49.2500	7.4506	60.5000	8.2499
38.2500	6.4307	49.5000	7.4708	60.7500	8.2654
38.5000	6.4570	49.7500	7.4909	61.0000	8.2807
38.7500	6.4831	50.0000	7.5109	61.2500	8.2959
39.0000	6.5090	50.2500	7.5307	61.5000	8.3110
39.2500	6.5348	50.5000	7.5504	61.7500	8.3261
39.5000	6.5604	50.7500	7.5700	62.0000	8.3410
39.7500	6.5860	51.0000	7.5895	62.2500	8.3559
40.0000	6.6114	51.2500	7.6089	62.5000	8.3707
40.2500	6.6366	51.5000	7.6281	62.7500	8.3853
40.5000	6.6617	51.7500	7.6473	63.0000	8.3999
40.7500	6.6865	52.0000	7.6663	63.2500	8.4144

TABLE 1 - CONT.
NOZZLE CONTOUR COORDINATES

X-INCHES	R-INCHES	X-INCHES	R-INCHES	X-INCHES	R-INCHES
63.5000	8.4288	74.7500	8.9923	86.0000	9.4119
63.7500	8.4431	75.0000	9.0031	86.2500	9.4199
64.0000	8.4574	75.2500	9.0138	86.5000	9.4277
64.2500	8.4715	75.5000	9.0244	86.7500	9.4356
64.5000	8.4856	75.7500	9.0349	87.0000	9.4433
64.7500	8.4995	76.0000	9.0454	87.2500	9.4510
65.0000	8.5136	76.2500	9.0558	87.5000	9.4587
65.2500	8.5272	76.5000	9.0662	87.7500	9.4662
65.5000	8.5412	76.7500	9.0764	88.0000	9.4738
65.7500	8.5546	77.0000	9.0867	88.2500	9.4812
66.0000	8.5683	77.2500	9.0968	88.5000	9.4887
66.2500	8.5816	77.5000	9.1069	88.7500	9.4961
66.5000	8.5952	77.7500	9.1169	89.0000	9.5034
66.7500	8.6082	78.0000	9.1269	89.2500	9.5106
67.0000	8.6217	78.2500	9.1367	89.5000	9.5179
67.2500	8.6348	78.5000	9.1466	89.7500	9.5250
67.5000	8.6478	78.7500	9.1563	90.0000	9.5321
67.7500	8.6608	79.0000	9.1660	90.2500	9.5392
68.0000	8.6737	79.2500	9.1756	90.5000	9.5462
68.2500	8.6865	79.5000	9.1852	90.7500	9.5531
68.5000	8.6992	79.7500	9.1947	91.0000	9.5600
68.7500	8.7118	80.0000	9.2041	91.2500	9.5669
69.0000	8.7244	80.2500	9.2134	91.5000	9.5737
69.2500	8.7369	80.5000	9.2227	91.7500	9.5804
69.5000	8.7493	80.7500	9.2320	92.0000	9.5871
69.7500	8.7616	81.0000	9.2412	92.2500	9.5938
70.0000	8.7738	81.2500	9.2503	92.5000	9.6003
70.2500	8.7860	81.5000	9.2593	92.7500	9.6069
70.5000	8.7981	81.7500	9.2683	93.0000	9.6134
70.7500	8.8101	82.0000	9.2773	93.2500	9.6198
71.0000	8.8221	82.2500	9.2861	93.5000	9.6262
71.2500	8.8339	82.5000	9.2949	93.7500	9.6326
71.5000	8.8457	82.7500	9.3037	94.0000	9.6389
71.7500	8.8574	83.0000	9.3123	94.2500	9.6451
72.0000	8.8691	83.2500	9.3210	94.5000	9.6513
72.2500	8.8806	83.5000	9.3295	94.7500	9.6575
72.5000	8.8921	83.7500	9.3380	95.0000	9.6636
72.7500	8.9035	84.0000	9.3465	95.2500	9.6696
73.0000	8.9149	84.2500	9.3549	95.5000	9.6757
73.2500	8.9262	84.5000	9.3632	95.7500	9.6816
73.5000	8.9374	84.7500	9.3715	96.0000	9.6876
73.7500	8.9485	85.0000	9.3797	96.2500	9.6934
74.0000	8.9595	85.2500	9.3878	96.5000	9.6993
74.2500	8.9705	85.5000	9.3959	96.7500	9.7050
74.5000	8.9814	85.7500	9.4040	97.0000	9.7108

TABLE 1 - CONT.
NOZZLE CONTOUR COORDINATES

X-INCHES	R-INCHES	X-INCHES	R-INCHES	X-INCHES	R-INCHES
97.2500	9.7165	108.5000	9.9290	119.7500	10.0696
97.5000	9.7221	108.7500	9.9328	120.0000	10.0721
97.7500	9.7277	109.0000	9.9366	120.2500	10.0745
98.0000	9.7333	109.2500	9.9404	120.5000	10.0769
98.2500	9.7388	109.5000	9.9441	120.7500	10.0793
98.5000	9.7442	109.7500	9.9478	121.0000	10.0816
98.7500	9.7497	110.0000	9.9515	121.2500	10.0840
99.0000	9.7550	110.2500	9.9551	121.5000	10.0863
99.2500	9.7604	110.5000	9.9587	121.7500	10.0885
99.5000	9.7657	110.7500	9.9623	122.0000	10.0908
99.7500	9.7709	111.0000	9.9658	122.2500	10.0930
100.0000	9.7761	111.2500	9.9693	122.5000	10.0952
100.2500	9.7813	111.5000	9.9727	122.7500	10.0974
100.5000	9.7864	111.7500	9.9761	123.0000	10.0996
100.7500	9.7915	112.0000	9.9795	123.2500	10.1017
101.0000	9.7965	112.2500	9.9829	123.5000	10.1038
101.2500	9.8015	112.5000	9.9862	123.7500	10.1059
101.5000	9.8065	112.7500	9.9895	124.0000	10.1080
101.7500	9.8114	113.0000	9.9928	124.2500	10.1101
102.0000	9.8162	113.2500	9.9960	124.5000	10.1121
102.2500	9.8210	113.5000	9.9992	124.7500	10.1141
102.5000	9.8258	113.7500	10.0024	125.0000	10.1161
102.7500	9.8306	114.0000	10.0055	125.2500	10.1181
103.0000	9.8353	114.2500	10.0086	125.5000	10.1200
103.2500	9.8399	114.5000	10.0117	125.7500	10.1220
103.5000	9.8446	114.7500	10.0147	126.0000	10.1239
103.7500	9.8492	115.0000	10.0178	126.2500	10.1258
104.0000	9.8537	115.2500	10.0207	126.5000	10.1277
104.2500	9.8582	115.5000	10.0237	126.7500	10.1296
104.5000	9.8627	115.7500	10.0266	127.0000	10.1315
104.7500	9.8671	116.0000	10.0295	127.2500	10.1334
105.0000	9.8715	116.2500	10.0324	127.5000	10.1353
105.2500	9.8758	116.5000	10.0353	127.5844	10.1359
105.5000	9.8801	116.7500	10.0381		
105.7500	9.8844	117.0000	10.0408		
106.0000	9.8887	117.2500	10.0436		
106.2500	9.8929	117.5000	10.0463		
106.5000	9.8970	117.7500	10.0490		
106.7500	9.9011	118.0000	10.0517		
107.0000	9.9052	118.2500	10.0543		
107.2500	9.9093	118.5000	10.0569		
107.5000	9.9133	118.7500	10.0595		
107.7500	9.9173	119.0000	10.0621		
108.0000	9.9212	119.2500	10.0646		
108.2500	9.9251	119.5000	10.0671		

```
ΔASSIGN S=MTO,BI=CR.
ΔFØRTLØAD BIU.
```

APPROVAL

DESIGN OF A MACH 8.0 AXISYMMETRIC NOZZLE FOR
A HYPERSONIC TEST FACILITY

by

Joseph L. Sims and Robert F. Elkin

The information in this report has been reviewed for security classification. Review of any information concerning Department of Defense or Atomic Energy Commission programs has been made by the MSFC Security Classification Officer. This report, in its entirety, has been determined to be unclassified.

This document has also been reviewed and approved for technical accuracy.

W. Dahm

W. K. DAHM
Chief, Aerophysics Division

E. D. Geissler

E. D. GEISSLER
Director, Aero-Astrodynamics Laboratory

☆U. S. GOVERNMENT PRINTING OFFICE: 1972—740-386/4102

DISTRIBUTION

DIR
DEP-T
A&TS-PAT
PM-PR-M, Mr. Goldston
A&TS-MS-H
A&TS-MS-IP
A&TS-MS-IL (8)
A&TS-TU, Mr. Wiggins (6)

S&E-AERO-R, Mrs. Hightower

<u>S&E-AERO-DIR</u>
Dr. Geissler
Mr. Horn

<u>S&E-AERO-A</u>
Mr. Dahm
Mr. Holderer
Mr. Felix
Mr. J. Davis
Mr. Gwin
Mr. Simon
Mr. Struck
Mr. D. Andrews
Mr. J. Johnson
Mr. K. Blackwell
Mr. Ramsey
Mr. J. F. Sims
Mr. Dunn
Mr. Henson
Mr. Bacchus
Mr. H. Wilson
Mr. Greenwood
Mr. D. Seymour
Mr. Forney
Mr. Dash
Mr. R. Elkin
Mr. T. Reed
Mr. Warmbrod
Mr. J. L. Sims

Scientific & Technical Info Facility (25)
P. O. Box 33
College Park, Md 20740
ATTN: NASA Rep (S-AK/RKT)